

ELIMINATION OF FLOW-INDUCED INSTABILITY FROM STEAM TURBINE CONTROL VALVES

by

Jim Hardin

Senior Engineer

Frank Kushner

Senior Consulting Engineer

Elliott Turbomachinery Company Inc., Ebara Group

Jeannette, Pennsylvania

and

Stephen Koester

Reliability Engineer

The Dow Chemical Company

Hahnville, Louisiana



Jim Hardin is a Senior Engineer in the Advanced Technology department at Elliott Company, in Jeannette, Pennsylvania, where he performs computational fluid dynamics (CFD) and other aerodynamic analyses for turbines and compressors. Previous experience includes CFD and other analyses on shipboard propulsion and piping systems with Westinghouse Electric Corporation, and turbine design support and testing at Elliott Company. He

has 22 years of engineering experience, mostly in aerodynamics and fluid systems.

Mr. Hardin received a B.S. degree (Mechanical Engineering, 1981) from Carnegie-Mellon University, and is a registered Professional Engineer in the State of Pennsylvania.



Frank Kushner is a Senior Consulting Engineer for dynamics and acoustics testing at Elliott Company, in Jeannette, Pennsylvania. He has 34 years' experience with industrial turbomachinery, and four years' previous experience with the combustion section development group at Pratt and Whitney Aircraft. He is a previous author for the Ninth, Twenty-Fifth, Twenty-Ninth, and Thirty-First Turbomachinery Symposia, as well as for ASME.

After obtaining a B.S. degree (Mechanical Engineering, 1965) from Indiana Institute of Technology, Mr. Kushner received his M.S. degree (Mechanical Engineering, 1968) from Rensselaer Polytechnic Institute. He is a registered Professional Engineer in the State of Pennsylvania and a member of ASME and the Vibration Institute. Mr. Kushner holds patents for a blade damping mechanism and a method to prevent one-cell rotating stall in centrifugal compressors.

Stephen Koester is a Reliability Engineer with 13 years of experience with Union Carbide/The Dow Chemical Company, in Hahnville, Louisiana. During his first 11 years, he worked as an Area Mechanical Engineer in Technical Services supporting Olefins I & II and Distribution facilities. During this time, he

experienced major turnarounds in 1989, 1992, and 1998, and has a broad background in performance and operations of the turbomachinery in both plants. He has been responsible for turbomachinery repair and reliability. During 1995, he took part in supporting a modernization of Olefins I turbomachinery. During the last two years, he has been assigned as the Reliability Engineer for both the Olefins Plants.

Mr. Koester received a B.S. degree (Mechanical Engineering, 1989) from Louisiana Tech University.

ABSTRACT

This paper describes two steam turbine governor valve failures in the same installation, the troubleshooting that determined the root cause, and the new valve designed to prevent similar failures. The original governor valve design had been used successfully for many years in large multistage, multivalve steam turbines, but apparently was not reliable at the high steam pressures employed today. Mechanical analyses, flow analyses, and testing showed that the failures were caused by flow-induced instability in the valve. Candidate valves with more stable flow fields were designed and tested. The final design combined features of two other, more typical designs, and showed good flow stability throughout the lift range. This new "hybrid" valve has since been applied successfully in other turbines.

INTRODUCTION

Steam turbine control valves are generally a high source of noise, as described by Araki, et al. (1981), Heymann and Staiano (1973), and others. Vibration of the valves can sometimes induce failures, as described by Johns, et al. (1997). Typically, the high noise occurs mostly at high pressure drop, with or without shock waves, but reliability is not an issue. Most steam turbines do not operate with valves just off their seats, a position that generally gives the highest pressure pulsations and noise.

Typical turbine steam chest pressures and temperatures have risen in recent years, from about 1450 psig and 900°F to as much as 2000 psig and 1000°F. With the same governor valve designs being applied at higher steam chest pressures, there is potential for the destructive effects of valve vibration to be magnified. Valves that were reliable in many applications for many years might turn out to be inadequate for the new, higher pressures.

In 1999, analysis of a reported control valve failure was initiated, eventually requiring both analytical and specialized

testing to solve the problem. The steam chest conditions were approximately 1650 psig and 860°F. The steam turbine has a sequencing valve rack to provide full admission at full load. The lift bar, valve rack, and mating valve seats are shown in Figure 1, with the valves in the closed position. As the lift bar is lifted and each valve gets closer to nearly full-open position, the next valve starts to open, so there is overlap.

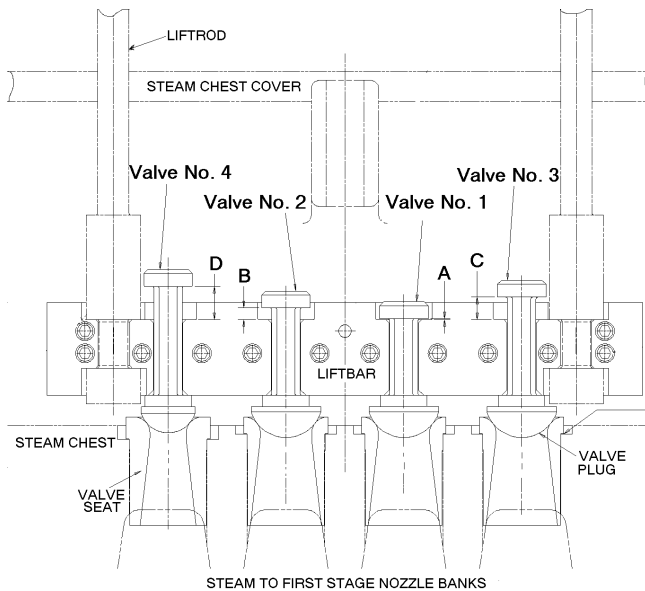


Figure 1. Valve Rack in Closed Position Showing Initial Clearances, A Through D.

The turbine is in a petrochemical-manufacturing complex started up in 1966, converting petroleum-based raw materials into a wide variety of basic building block and intermediate chemicals. The facility manufactures more than eight billion pounds of chemicals for customers worldwide. The Star plant, which began operations in 1981, produces polyethylene used in a wide range of plastic products worldwide. The ethylene expansion plant was modernized in 1998. The subject turbine was one of the new steam turbine compressor drivers added at this time.

After about three months of operation, the first failure on valve No. 2 was reported to occur when valve No. 3 started to open. The turbine was running at 3100 rpm. A large hammering noise existed prior to the failure. Valve No. 2 was not at low lift with high pressure drop, but rather at about 20 percent lift, which is near its cutout lift, at approximately 5 percent pressure drop. Valve No. 1 was nearly fully lifted, and valve No. 3 had started to lift. After valve No. 2 failed, the rack was immediately opened to adjust for flow/load with control operation on valve No. 4, having valves No. 1 and 3 nearly open. The turbine was kept running with the known valve failure.

Prior to this failure, plant startup had higher noise, so chattering might have existed prior to failure. It was confirmed that the unit had quickly run through the valve No. 1 opening sequence due to flow available. Consequently, valve No. 1 might not have been in the 20 percent lift position for very long, perhaps explaining why the high vibration and noise observed for valve No. 2 was not seen for valve No. 1. Operation was primarily with valves No. 1 and 2. As more process furnaces were added, valve No. 3 started to open and valve No. 2 failed. There was no vibration reported for valve No. 4 for the next two months of operation.

When the steam turbine was taken apart, it was found that the plug portion of valve No. 2 had broken off and had driven the seat into the steam chest wall approximately 0.7 inch. It was very surprising that the valve failed near the plug (Figure 2). As the lift bar moves through the clearances A through D shown in Figure 1,

lifting the valves, the support point of each open valve is near the top of the stem. If there were only cantilevered bending involved, the maximum stress would be near the support point. The fretting on the valve stem surfaces shown in Figure 3 indicated that the valve plug was vibrating so much that it was exceeding the clearance between the sides of the stem and lift bar, with maximum bending stress near the bottom instead of near the top of the stem, where it is held by the lift bar. The stem cross section is rectangular, to prevent spinning of the valve. (Piping strain on the casing also had to be corrected during the shutdown, and it was found that the rotor rubbed during a vibration excursion from a rotor bow.)

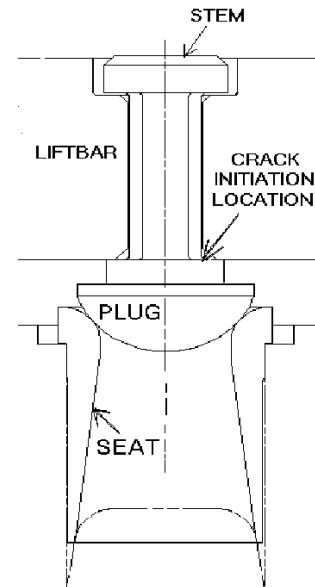


Figure 2. Valve in Closed Position Showing Initiation Point for Fatigue Crack.

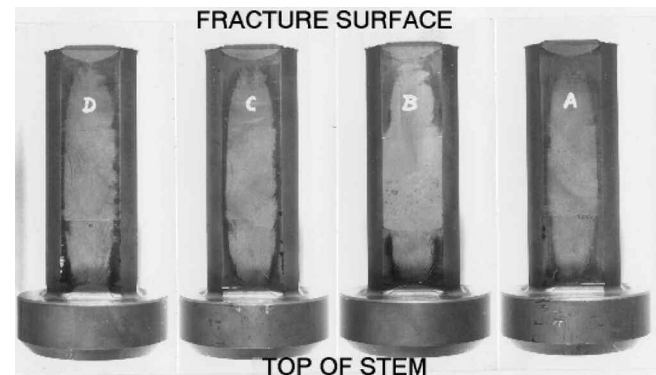


Figure 3. Valve Failure with Evidence of Rotating Bending from Fretting Pattern Found on All Four Sides of Stem.

The turbine was repaired and reassembled with a "Mod 1" valve design. These new valves were made from valves of the original design by machining a countersink in the bottom of each plug, as shown in Figure 4. After the Mod 1 valve plugs were installed, a second failure occurred, but this time it was valve No. 1 that failed when it was near its cutout lift and valve No. 2 was beginning to open, similar to the situation with valve No. 2 during its earlier failure. Operating speed was higher, near 3500 rpm, and a large hammering noise existed prior to the failure. The turbine had started to shake immediately during startup while running with the valve rack lifted 32 percent, and had continued for 50 minutes until valve No. 1 failed. The noise was likened to one's vehicle tires traversing rumble strips. The term "rumble-strip vibration" was thus used to refer to this severe vibration.

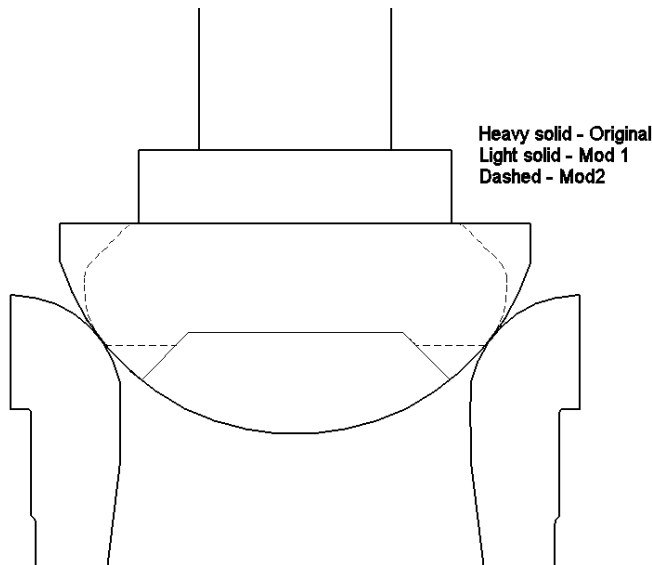


Figure 4. Cross Section Through Valve Showing Original and Modified Plug Shapes.

After the failure, operation continued for about a day on valve No. 2 before shutdown to complete furnace repairs and install another modified valve. During this day of operation, valve No. 2 was making a mild noise between 51 and 60 percent open (with failed valve No. 1 shut). When inspected, valve No. 2 had no cracks, its seat was not damaged, and there were no cracks in tack welds holding the seat to the steam chest. This and other evidence proved that the failures were not due to impacts between the plug and seat. This second failure resulted in the broken-off plug of valve No. 1 pushing the seat into the chest more than an inch. Later, inspection of the plug and seat surfaces' extruded metal flow proved that the impact of the seat was a one-time event. It had also been reported that the unit was going in and out of vibration, coinciding with raising the servomotor to increase flow, power, and speed, and cutting in valve No. 2. Restart had been with full inlet pressure.

After the Mod 1 valve failed, a second revision, Mod 2, was installed (also requiring a modified lift versus area curve). These valves were made from Mod 1 valves and were similar to another valve design with which the turbine manufacturer had success in the past. The Mod 2 plug shape is shown in Figure 4. Due to damage to the steam chest, the new valve No. 1 had to be made longer so it could reach the seat. It was also decided to run with inlet pressure reduced by 12 percent. These Mod 2 valves remain in operation with mild vibrations at times, but have not failed, and there have been no severe extended "rumble-strip" vibrations. A plant shutdown to install a new "hybrid valve" design to replace the Mod 2 valves has been delayed. Even though other changes were made to reduce risk of a third failure, the steam turbine has been operating for approximately three years with the undesirable vibration. A short-term fix shown in Figure 5, with dynamic stresses reduced by a factor of three, was also designed and supplied in case there was a third failure.

In the meantime, extensive computational fluid dynamics (CFD) analyses and rig tests were used to eventually develop hybrid valves described later in this paper. The following sections describe the failure analysis, as well as the analysis and testing of the new hybrid valves that have been successfully applied in other turbines to eliminate the vibration at high lift points.

FAILURE ANALYSIS

Related Experience

Previous problems with valve flow instability had occurred at low lifts, and had been solved with changes to the contour of the

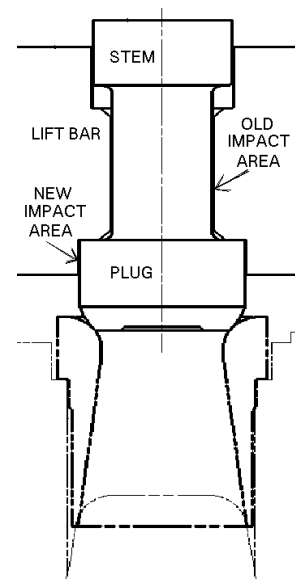


Figure 5. Stronger Plug and Stem Design with Mod 2 Plug Shape.

valves and seats. The report of the first valve failure in the current turbine was surprising in that the valve was reported to be lifted well off its seat, with a low pressure drop of only about 5 percent across the valve. Moreover, there were no reports of problems for a nearly identical valve rack at another plant, operating with similar inlet steam conditions for about one year. Many other units had similar rack/valve/seat designs of different sizes, along with various steam inlet flows, temperatures, pressures, and operating speeds. One of these units had two valves of same size as those in the failed turbine with no reports of problems for five years. However, unusually high valve noise levels occurred after an uprate that included two additional same-size valves; valve lift points with high noise were avoided by using the trip and throttle (T&T) valve. The turbine with failed valves had system pressure control that precluded continuous T&T valve control operation. The failed unit was at the upper end of design steam inlet conditions, so initial review focused on design limitations.

Vibration Data Analysis and Dynamics Lab Testing

Initial data obtained in the field was with accelerometers that were helpful, but concurrent pressure pulsation data from ports downstream of the valves, shown in Figure 6, were deemed at first to be useless. Pressure pulsations at high amplitudes in the frequency range of 250 to 500 Hz were eventually shown to be due to "organ pipe" resonance due to probes not being flush-mounted. "Organ pipe" is a term used for longitudinal acoustic modes of tubes using calculations shown in APPENDIX A. However, laboratory testing discussed in APPENDIX A clarified what data were useful from the pressure probe measurements, and more field tests during valve vibration after the second valve failure correlated with analysis and valve rig tests to prove the cause of vibration. Data were obtained for Mod 2 valve No. 2 for valve rack lift near 58 percent opening, showing the occurrence of severe vibration in the 30 to 40 Hz frequency range. For these tests, transient data were obtained with a tape recorder for laboratory analysis. Indeed, listening with a speaker connected to the tape recorder output of the dynamic pressure probe sounded similar to a vehicle traveling over rumble strips, as the observed sound from the valves had been described earlier.

In Figure 7 is shown the frequency spectrum for the pressure port transducer downstream of valve No. 2 just before there was severe vibration. At other valve lifts, the high amplitudes near 350 Hz sometimes reached ± 400 psi due to the "organ pipe" resonance described in APPENDIX A. Analysis of pulsation frequencies gave

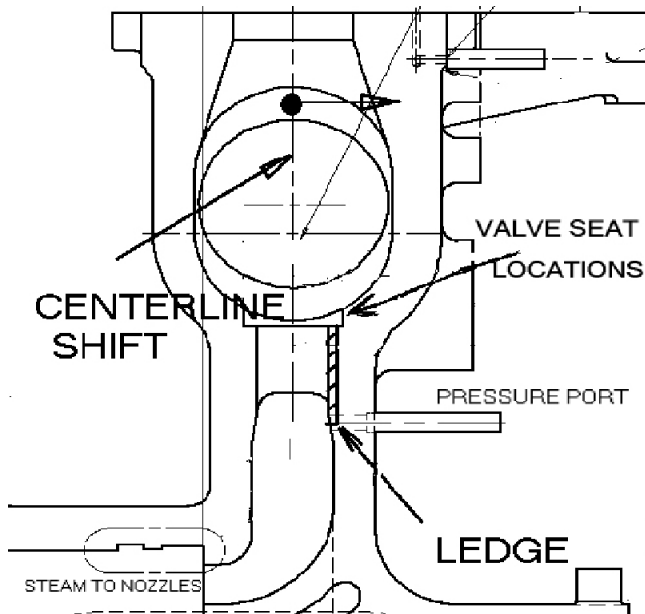


Figure 6. Side View of Steam Chest Downstream of Valves Showing Machined-In Ledge at Pressure Ports Leading to Pressure Transducers.

a variation for all four of the pressure ports, with amplitude decreasing as a particular valve lifted, that is, velocity decreases along the wall giving lower excitation at the port entrances. There is a backward-facing step from the end of the valve seats that also causes variations. The change in frequency, however, was conclusively shown to be due to differences in the water leg in the piping between the port entrance and the transducer. Another verification test was also done using a steam vent in the instrument line, which completely modifies the open-closed configuration with an open branch, with the frequency changing from 235 Hz to 320 Hz when venting steam.

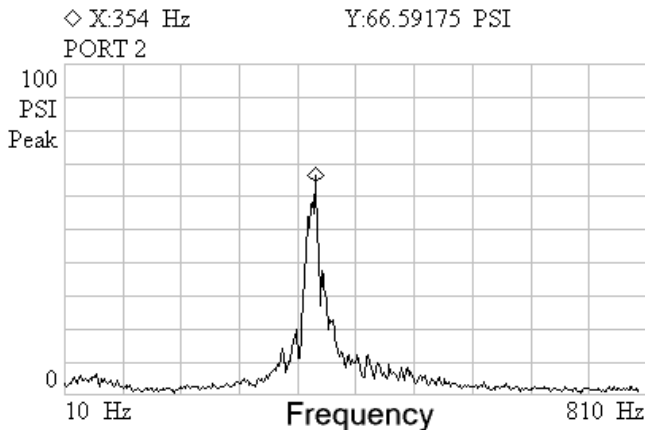


Figure 7. Pressure Pulsations at Port 2 Before High Vibration of Valve No. 2.

In Figure 8 is a long time trace period of four seconds showing intermittent high “rumble-strip” vibration. By using this time scale, the result filters out the high frequencies, including the “organ pipe” resonance for the port frequency near 350 Hz. The high amplitude changes are occurring at a rate between 30 and 40 Hz. Since the frequency of the sharp pulses near 35 Hz is well below 350 Hz, amplitudes should be accurate, just as is the static pressure. Zooming in with a quarter-second time window shows extremely high changes in pressure at a rate of 30 to 40 Hz, as

shown in Figure 9, an amplitude versus time trace, and Figure 10, a typical spectrum plot. The character of the pulsations is complex, and there appears to be a beating effect since the high frequency content shows a tremendous pulsation amplitude at frequencies near both 350 and 385 Hz. Beating occurs when an excitation frequency is near a natural frequency, with response for each frequency. One of the frequencies could be the port frequency or the valve “hanging mode” frequency, that is, the frequency of the fundamental bending mode with the valve stem supported by pressure loads clamping it to the lift bar. The difference in frequencies, 30 to 40 Hz, can be seen in the plots, and is the rate of the “rumble strip” vibration. This was deemed to be the rate that the valve stem was slamming against the lift bar in a rotating fashion, causing the fretting shown in Figure 3. In addition, with a rotating pressure field from the flow instability, the flow past the entrance to the port would be very erratic. The sharp changes at 30 to 40 Hz are such that there is high harmonic content, including nine and 10 times, that is in the range of the “hanging mode” natural frequencies of the valve at that lift point. The response would be amplified for both valve frequencies that are close together for the two transverse directions for a cantilever.

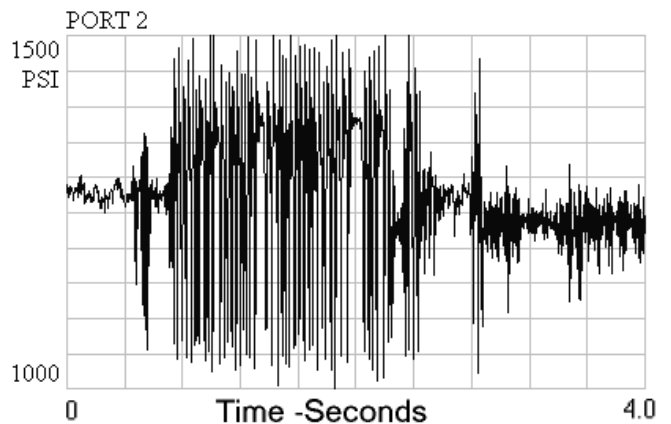


Figure 8. Time Trace of Port 2 Pressure Pulsations During Vibration Transient.

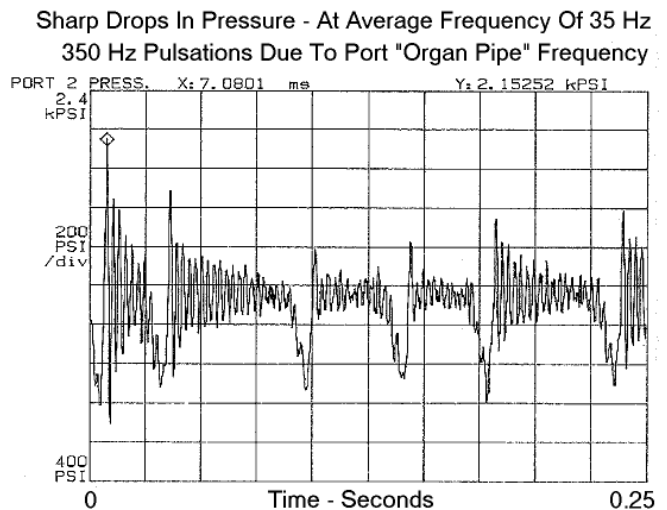


Figure 9. Port 2 Pressure Pulsations During High Valve Vibration.

It was also found that when the “rumble-strip” vibration commenced, there was an instantaneous lift of the lift bar. To eliminate controls as the cause, the controller was set at a manual set point. The lift bar still tried to lift vertically, and the quick lift still occurred. Thus, the most probable cause of the quick vertical lift of the entire lift bar is that at the onset of aerodynamic

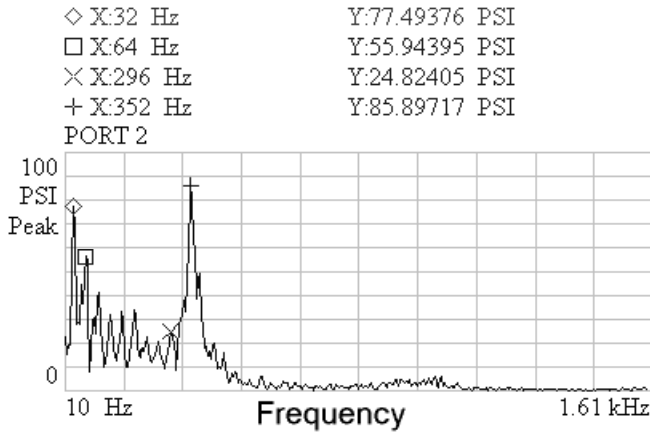


Figure 10. Port 2 Pressure Pulsation Frequency Spectrum During High Valve No. 2 Vibration.

instability at the valve, there is a large drop in average reaction force vertically, lowering the force required from the servomotor. There also was a simultaneous increase in static pressure downstream of valve No. 3 as the bar lifted, also decreasing the force required from the servo linkage.

At the same instant that valve No. 2 was experiencing severe vibration, there was no sign of the 30 to 40 Hz pulsations downstream of the other valves. Also, with higher flow, data with valve No. 3 cutting out and the next valve, No. 4, cutting in did not show any vibration and pressure pulsations in the 30 to 40 Hz range. Pulsations due to “organ pipe” resonance downstream of valve No. 3 were just as high in amplitude, and over time in the same frequency range, so that itself was not the direct cause of initiation of severe vibration. This confirmed reports that valve No. 3, despite being identical to Nos. 1 and 2, never vibrated. There was no definitive explanation for this difference in behavior. One possibility is the presence of water ingestion, which can occur with superheated steam as described by Feray (1999). The potential for water could have been eliminated as more furnaces came online and total flow steadily increased, with a dry system by the time valve No. 3 was cutting out. Another possibility is that the flow pattern was somewhat different due to location in the steam chest, side clearances, and variations from the machined-in ledge downstream of the valves as shown in Figure 6, due to an inadvertent casting shift. A third possible cause is that pressure port “organ pipe” frequencies were found to be somewhat different during testing. The frequency range was coincidentally near the valve fundamental natural frequency (hanging mode) described below. There would be some acoustic excitation of the valves, but laboratory tests showed that pressure pulsations would be low, as explained in APPENDIX A. Calculated acoustic pressure of 5 psi would have to be amplified by a factor of 250 to reach the calculated stress level from fracture mechanics analysis. In addition, the sound traveling as a plane wave would encompass the valve plug instead of being high positive on one side and out of phase 180 degrees away. However, the acoustic pulsations could have acted as a trigger to induce high vibration only for valve Nos. 1 and 2, but may have been much farther from the natural frequency of valve No. 3.

Valve Natural Frequency Analysis and Testing

Initial frequency testing of a spare valve was with a clamping mechanism, with final tests using a flexible fixture to hydraulically push the top of the stem against the lift bar to simulate clamping from steam pressure drop across the valve. For the final test, the pressure load existing during failure was simulated with a force equal to that from steam differential forces. In addition, finite element analysis (FEA) was also used to show that the effect of the lift bar on valve natural frequencies was small. In Table 1 are

shown results for various pressure loads. As is normal, there are two frequencies close together for the two transverse directions perpendicular to the valve. The load case of 1325 lb is that for the valve lift condition with severe vibration; frequency drops as the valve is lifted farther, giving a smaller clamping force. The frequencies at temperature would be 10 percent lower due to reduced modulus of elasticity. Valve frequencies for original versus modified plugs would vary somewhat due to differences in stem lengths and mass. Testing and calculations for the lift bar mechanism gave average frequencies of 35 and 45 Hz for the two transverse directions, and near 100 Hz for the vertical direction, with some variation from closed to full open position as the lift rods change support length. These lift bar frequencies had margin from operating speed. Furthermore, they were not a direct cause of the high valve vibration observed, since data verified that when a particular valve vibrated, the others did not show response.

Table 1. Original Valve Natural Frequency Variation with Pressure

Pressure Load Lbs	Bending Mode Freq. Hz	Torsion Mode Freq. Hz
325	208/238	850/930
675	268/282	1050/1160
1325	290/310	1200/1240

Load Holding Valve to Lift Bar.

Stress and Fracture Mechanics Analysis

An extensive fracture mechanics analysis was done for the valve plug from the second failure, including striation spacing measurements with a transmission electron microscope. The appearance of crack surfaces suggested that the crack initiation and the subsequent crack growth were due to a rotating bending moment (that is, simple lateral bending but with the direction of bending rotating on the valve axis). This conclusion is important because it agrees with the driving mechanism to be described later in the CFD analysis. In Figure 11 is shown a crack surface with multiple initiation sites around the entire circumference and a final fracture area (with rough appearance) displaced somewhat from the center of the plug. The final fracture area for the first valve failure was more centered, perhaps due to more equal clearances on the four sides of the stem. The critical crack size was estimated for the final fracture. The axial force due to the differential pressure across the valve was less than 11,000 lb, resulting in an axial tensile stress in the critical cross section below 4 ksi. However, the stress necessary to initiate and grow fatigue cracks in the critical cross section is much higher, so the rotating bending moment was still present at the time of final fracture. It was also concluded that the stress induced by the differential pressure is subjected to a relatively small number of fluctuations, and therefore the direct axial load was not contributing significantly to the fatigue damage of the valve. Thus, the source of the bending moment resulting in a high bending stress in the critical cross section also drove the fatigue crack initiation and subsequent crack growth.

Traditional stress analysis was first used to determine when the maximum nominal bending stress in the uncracked ligament exceeded the ultimate strength of the AISI 422 stainless steel material, 118,000 ksi near 900°F. Such a stress can be induced by the bending moment, which was calculated to be 12,800 in-lb for the dimensions of the final fracture cross section. The nominal bending stress at the crack initiation site in the uncracked cross section induced by the same bending moment was then calculated to be 20.2 ksi. With this high stress just before the final fracture, there should have been some plastic deformation in the uncracked ligament, but none was found. It may have been that the bending moment was lower at the instant of final fracture. However, in order to attain such a high nominal stress in the uncracked ligament, significant plastic deformation should occur prior to the final fracture. Macroscopic observations of the fracture surfaces,

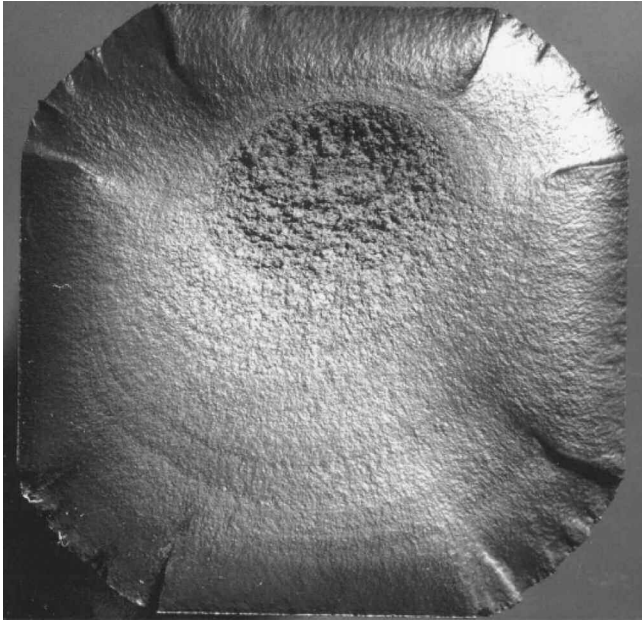


Figure 11. Fracture Surface of Second Failure, Valve No. 1 Mod 1, with Smooth Fatigue Surfaces (Rough Surface Was Final Fracture Area).

visible on the two failed valves, led to the conclusion that the final fracture of the remaining ligament was not predominantly plastic. Therefore, a second calculation of the critical stress at the final fracture was obtained from the fracture mechanics analysis method given by Glinka and Newport (1987) and Glinka and Shen (1991).

The critical stress intensity factor for AISI 422 steel was estimated as $K_{Ic} = 90 \text{ ksi-in}^{-1/2}$. The calculation of stress intensity used the weight function method for a single edge crack in a rectangular cross section. The stress distribution was determined using the stress concentration factor from FEA analysis and the universal notch tip stress distribution fields. The stress intensity factor, K , was calculated as $K = S (\Pi \cdot a)^{1/2} \cdot Y$; where S is applied stress, a is crack length, and Y is a correction factor dependent on geometry of sample, type of crack, and loading conditions.

Knowing that the critical stress intensity is $90 \text{ ksi-in}^{-1/2}$, the nominal bending stress was calculated to be 18.3 ksi. Because the critical stress at the final fracture was induced by bending moment for a stress of 18.3 ksi, this also had to be the fluctuating stress for the entire fatigue stress cycle.

Finally, the crack surface itself was examined with a transmission electron microscope and striation spacings were measured for various crack lengths. Actual test data were generated at temperature for the material to obtain fatigue crack growth rates, which were then used to predict the number of cycles with fracture mechanics equations such as in Kurihara, et al. (1987). The data showed that the nominal stress was in the range of 39 to 44 ksi. After including stress concentration effects, predicted number of cycles to crack initiation was only 1500 cycles. The cycles (one cycle per striation) were counted from average striation measurements at three crack lengths, giving crack propagation of roughly 130,000 cycles. The FEA model was also used to predict the dynamic stresses from "rumble-strip" vibration when the stem was slammed against the bar, giving the fretting condition in Figure 3. Using an estimated alternating sinusoidal pressure load of 1100 lb, the calculated stress correlated well with fracture mechanics results when using an impact multiplier between two and three. Thus, the crack initiation excitation mechanism calculated by three different methods described also showed that rotating bending moment had to be very high from some unknown mechanism. CFD and full scale rig testing then determined the mechanism.

Flow Analysis

Computational Fluid Dynamics

CFD analyses of a similar steam chest were available from previous work. These showed that the configuration of the steam chest had little effect on the flow field through each valve. Flow velocities in the steam chest were low enough that flow entering a valve distributed itself into a flow field that was nearly radially symmetrical, with practically no influence from adjacent valves or the steam chest geometry. This simplified following CFD analyses of the valves themselves considerably, because it was not necessary to include the entire steam chest in the model of each valve.

CFD models of a single original-design valve at different lifts were built and run. Most of the models included one 90 degree section of the valve with periodic boundaries, which assumed that flow in the other three 90 degree sections was the same as that in the section that was modeled. The models were run steady-state rather than transient, which meant that the CFD analyses could not detect any flow transients or instabilities that might have caused the observed noise and failures. A proper transient model would have been much larger and run much more slowly, and it was considered unlikely that the CFD analyses could correctly predict the unstable flow effects anyway.

Steady-state pressure forces on the valve were calculated and passed to the stress analysts. These forces were parallel to the valve axis; the radial symmetry made all steady-state forces perpendicular to the valve axis sum to zero. The fluid flow also applied no significant torsion to the valve. Because the valve was a surface of revolution, there were no meridional surfaces for pressure forces to act on, whether steady-state or transient. Torsion was applied to the valve only through viscous friction, which was very small.

The CFD results also showed that flow in the valve throat was subsonic when the failures occurred, ruling out shock wave effects as the root cause.

Additional models and runs were made to evaluate the influence of an adjacent valve and to find the forces induced on the valve if it were off-center by the maximum tolerance in the mechanism. Both of these effects turned out to be insignificant.

Comparison with Technical Literature

Heymann and Staiano (1973) described the following two possible flow regimes through a valve:

- *Core flow*, in which flow between the plug and seat converges in the center of the flow passage under the plug and continues downstream in the middle of the passage. This type of flow is unstable and induces noise in a control valve.
- *Annular flow*, in which flow adheres to the seat walls, with reverse flow up the center of the seat to the plug. This type of flow is stable, and results in quieter valve operation.

CFD results of the original valve design showed strong core flow at the lifts analyzed, the type of flow considered unstable. Figure 12 shows predicted streaklines at 0.639 inch lift, the lift at which the failure occurred. The figure includes the valve plug and a cutaway view of the valve seat flow surface in the steam chest. The streaklines show the path of steam flowing between the plug and seat and downward through the venturi portion of the seat. The streaklines meet under the plug and fill the downstream passage, exhibiting core flow.

Araki, et al. (1981), found core flow in their baseline unstable valve and annular flow in their later improved valve. They developed geometric criteria for predicting whether a valve would be stable based on the radii of curvature of the valve plug and seat as seen in cross section. Their criteria predict the original-design valve analyzed here to be unstable, and indeed, their baseline valve

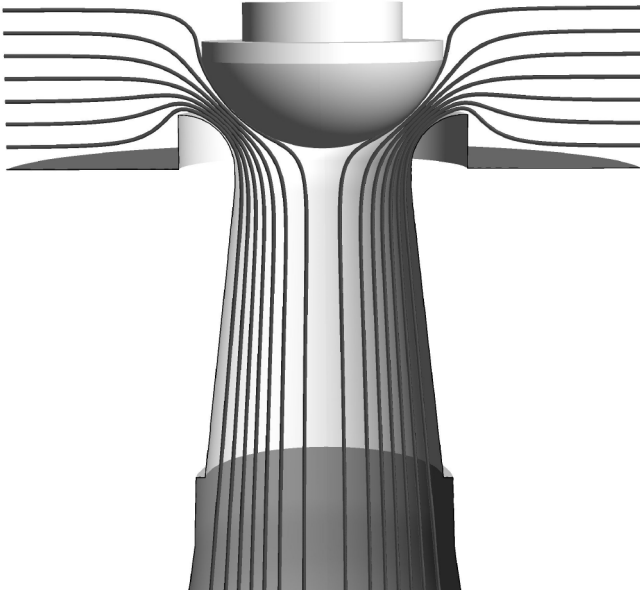


Figure 12. Original Valve with Flow Streaklines.

with unstable flow is similar to our original-design valve. Using the stability chart they developed for their baseline valve, one could predict that our similar original-design valve could have flow instabilities at all lifts greater than approximately 0.18 inch.

Using data from the Araki, et al. (1981), baseline valve, a likely worst-case momentary loading due to flow instability for the original-design valve was calculated and given to the stress analysts. This was the only significant force perpendicular to the valve axis that was calculated.

DETERMINATION OF ROOT CAUSE

None of the steady-state forces calculated for the valve stem were anywhere near large enough to account for the failure, so the failure mechanism had to involve transients. Analysis of the ordinary resonance effects on the valve also ruled them out as a root cause. The cause appeared to be a transient effect that standard analyses could not detect directly.

Possible failure causes that were studied and later ruled out as prime causes included control system problems, acoustic interaction with the steam chest cavities above and below the valves, resonant acoustic waves in the valve pressure ports, flow interaction between adjacent valves, and a double-throat instability between the valve and the turbine nozzles.

The shape of the original-design valve was similar to one known to have flow stability problems (Araki, et al., 1981), and the CFD analyses of this valve showed a core flow pattern known to be associated with flow instability (Heymann and Staiano, 1973). Furthermore, failure analysis on the valve stem showed bending perpendicular to the stem but with a rotating axis, consistent with unstable flow structures that would be free to rotate around the valve plug. Stress analysis showed that the order of magnitude of the transient forces from such a flow instability, estimated from the work of Araki, et al. (1981), might be sufficient to initiate a crack in the stem. All these pieces of evidence taken together led to the conclusion that flow-induced instability was the root cause of the valve failures.

At this point, the possibility still existed that the cause was a fluid-structure interaction leading to mechanical instability, as opposed to a strictly flow-induced instability. The technical literature implied this was not true; unstable flow structures were observed even in rigidly mounted two-dimensional sections of valves. Later testing, described below, ruled out the possibility of fluid-structure interaction.

VALVE DESIGN AND TESTING

Approach to Design

Based on what was seen in the CFD analyses and technical literature review, the basic approach to valve design was to try to make the flow field in the valve more annular. Also important was to ensure that the new valve would be easy to assemble or retrofit in the existing steam chest design. It was therefore required that a new valve seat fit in the same envelope as the original seat, and preferred to simply use the original seat design with a new valve plug, if possible. The new valve also had to have an opening-versus-lift characteristic that was reasonably linear and had no inflections or flat spots, so the control system would work well with it, and had to have only a single throat at all lifts, because double throats are known to lead to other kinds of flow instability. Further constraints were imposed for manufacturability and durability, including avoiding complex mechanisms and sharp edges.

CFD was used to evaluate how annular the flow field was at different lifts. Besides from subjectively reviewing the flow plots, two measurements of “annularity” were developed. The normalized flow radius, as a function of axial distance through the valve, was calculated as the mass-average of the radius from the valve axis divided by the radius of the flow passage. This measure approaches zero for strong core flow, one for strong annular flow, and is $\frac{2}{3}$ for uniform flow. The recirculation zone height is simply the distance from the bottom of the plug to the bottom of the flow recirculation zone below the plug. This measure approaches zero for strong core flow and tends to grow larger, with no particular upper limit, as flow becomes more annular. If used to compare valves of different sizes, it should be divided by a representative dimension, such as the venturi throat diameter.

Valve redesign began by using the geometric criteria described by Araki, et al. (1981), but also expanded to other methods to induce annular flow. Designs that showed promise were then tested at various lifts to confirm their stability.

Description of Tests

Tests were performed in a nitrogen blow-down facility at a contractor’s site using full-scale test valves. Because cool nitrogen was used instead of superheated steam, parametric similitude was used just in case the problem was a stability problem rather than a direct forcing function. The test valve was set to a particular lift and held there throughout the blow-down. The rig inlet valve was manually ramped open during the several seconds of blow-down, so the test valve inlet pressure was rising rapidly throughout each test. Steady-state conditions were never achieved. This arrangement led to too much data scatter to generate information on valve flow characteristics, but appeared to be sufficient to detect flow instability.

Later review of the data determined that the discharge piping was undersized, and was apparently choked most of the time. This caused the pressure ratio across the test valve to be fixed throughout each blow-down, despite the varying inlet pressure. Further analysis showed that the choked discharge piping had approximately the flow area of a typical turbine nozzle bank, so the test valve was operating at realistic conditions.

Instrumentation in the test rig included two proximity vibration probes on the valve stem and four dynamic pressure sensors at the seat venturi. Dynamic pressures showed flow instability directly; vibration showed the valve’s response to the flow instability.

The test rig was designed so that the natural frequency of the valve could be adjusted. The plugs could be mounted on valve stems of different diameters, and the length of the valve stem from the clamped support to the plug could be varied. Furthermore, the plug itself could be made of different materials with different densities.

Results

Original Plug

The first tests were performed on the original valve design. The authors were able to detect fluctuating pressures and valve vibration, as expected. Fourier analysis showed the frequency of the fluctuations to be roughly 100 Hz. The valve was tested again with a different stem length, and thus a different natural frequency, yet the same fluctuation frequency was found. This showed that the frequency of the pressure fluctuation was independent of the mechanical natural frequency. The pressure fluctuation was being caused by a strictly flow-induced instability, not a fluid-structure interaction. Therefore, mechanical changes to the valve or lift mechanism would not eliminate the root cause of the problem. The flow-induced instability would have to be addressed by changes to the flow path through the valve.

Cutoff Plug

The first alternative designs explored were based on the geometric criteria of Araki, et al. (1981). The plug was cut off abruptly shortly downstream of the plug/seal throat, to encourage flow separation from the plug and adherence to the seat wall. Such "cutoff" plugs were designed for both the original seat and a new seat with a larger seat wall radius. This category includes the Mod 2 plugs installed in the turbine after the second valve failure. Figure 13 shows a Mod 2 plug and the flow streaklines through it predicted by CFD. The flow is weakly annular at the lift shown. The black regions along the valve axis in the figure are where the flow is moving upward rather than downward, exhibiting the reverse flow up the center that occurs with annular flow.

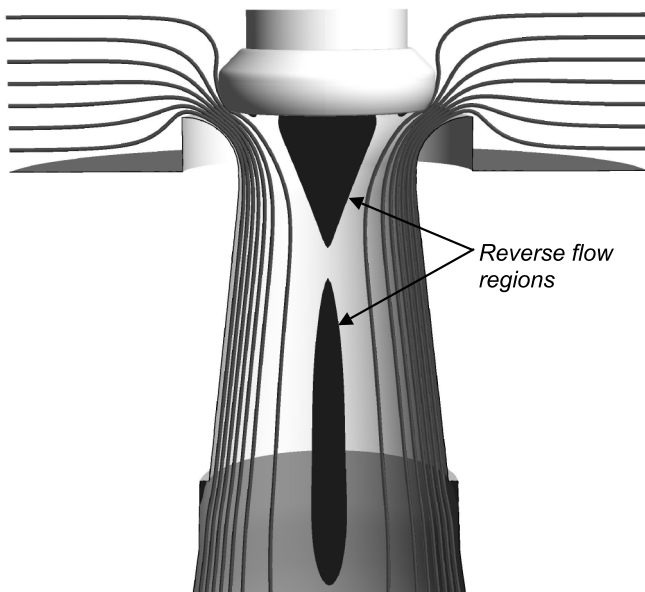


Figure 13. Cutoff (Mod 2) Valve with Flow Streaklines and Reverse Flow Regions.

CFD predicted strong annular flow at low lift, but with the annularity weakening and the central recirculation region dissipating at high lifts. Any valve will, of course, eventually lose annularity and transition to simple flow through a venturi as it opens wide enough, but it appeared the cutoff valves' loss of annularity might appear at too low a lift, perhaps affecting the lift at which the failures occurred. The large-radius seat did not appear to improve annularity significantly.

Test results did not confirm the trends seen with CFD. The cutoff valve with the original seat had significant pressure fluctuation at all lifts, similar to the original valve. Yet the cutoff valve with the large-radius seat had much lower pressure fluctuation at all lifts.

Concave Plug

The concave plug was designed to force flow explicitly downward along the seat walls in an annular flow field at high lifts, such as where the failures occurred. This plug, along with its predicted streaklines and reverse flow region at its design lift, is shown in Figure 14. The plug had a sharp corner like a cutoff plug, to force flow to separate from the plug once it was properly oriented. At lower lifts, however, the plug and seat formed a diverging passage. Flow followed the plug wall rather than the seat wall, so the flow was guided toward the center of the valve, encouraging core flow at low lifts. CFD predicted good annularity at high lifts, but core flow at low lifts. Test results confirmed this trend, showing low pressure fluctuation at high lift but high fluctuation at low lift.

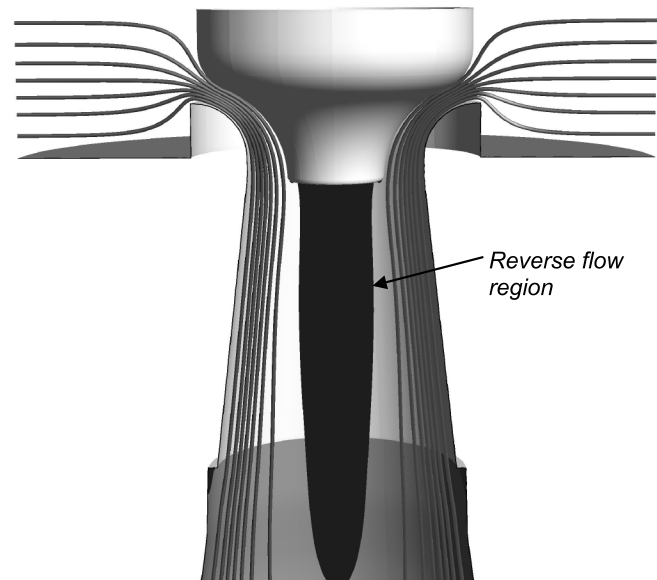


Figure 14. Concave Valve with Flow Streaklines and Reverse Flow Regions.

Hybrid Plug

Cutoff plug CFD results showed good annularity at low lifts but not at high lifts, and concave plug CFD results showed exactly the opposite trend. The hybrid plug, shown in Figure 15, was designed to combine the best features of each to achieve good annularity throughout the lift range. At low lift, the sharp corner on the plug behaves like a cutoff plug, with the additional benefit of upstream flow guidance into a downward-flowing annulus, like a concave plug. At high lift, the flow is shaped into an approximately downward annulus then separated from the plug sharp corner, like a concave plug. The plug sharp corner being located close to the seat wall encourages flow to adhere to the seat wall at all lifts. Figure 16 compares the flow fields of cutoff, concave, and hybrid valves predicted by CFD at low and high lifts. It shows that only the hybrid valve has strong reverse flow regions (the gray areas) at both low and high lift. The hybrid valve design is covered under international patent application PCT/US01/48091 and U. S. provisional patent application 60/245,100.

CFD predicted annular flow at both high and low lift. Test results confirmed this trend, showing low pressure fluctuation at all five lifts tested.

The hybrid plug was chosen as our new standard governor valve design. Although the hybrid valves have not been installed in the turbine that experienced the failures, they have been installed as original equipment in two other turbines. The valve racks were also modified to reduce valve stress, similar to the configuration shown in Figure 5. One turbine has been operating for over a year, the other for over two years. Neither has experienced a governor valve failure, and noise and vibration levels have not been excessive.

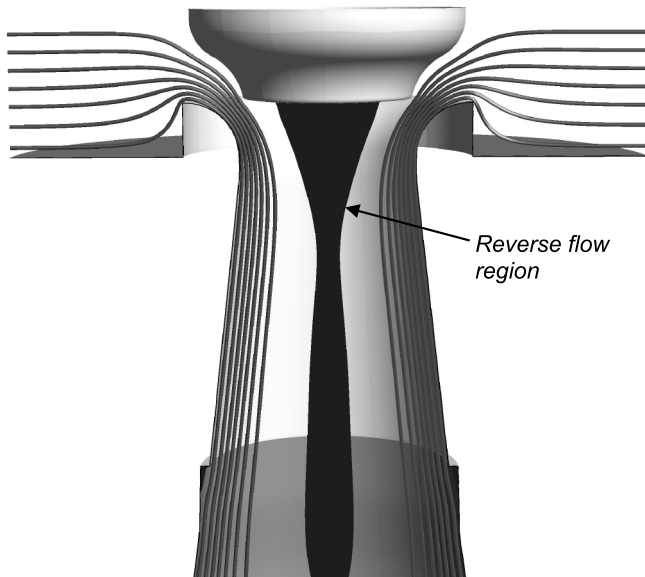


Figure 15. Hybrid Valve with Flow Streaklines and Reverse Flow Regions.

	Low Lift (same flow area)	High Lift (same flow area)
Cutoff Plug		
Concave Plug		
Hybrid Plug		

Figure 16. Comparison of Streaklines and Reverse Flow Regions in Valves.

FUTURE PLANS

The test rig used to evaluate candidate valve designs was not able to measure accurate steady-state flow versus pressure drop characteristics because of the continuously varying flow during each blow-down. Furthermore, excessive flow restrictions in the outlet piping prevented testing at pressure ratio and normalized flow combinations far from typical applications. Consequently, a major university has been engaged to build and operate a test rig

and find the complete flow and stability maps for the new valve. Additional instrumentation has also been specified for this new rig, to show more details of the flow instability. With these further insights, it might be possible to design a new governor valve that is even quieter and more stable.

CONCLUSION

The specific lessons learned from this case can be stated for turbine governor valves in general. As steam chest pressures on new turbines become ever higher, even governor valve designs with long application histories might be unable to operate reliably. A combination of fracture mechanics, FEA, CFD, rig tests, and field data is sometimes required to solve a problem. The source of the valve failures can be entirely flow-induced, independent of the mechanical characteristics of the valve. In such a case, changing the valve materials, mounting configuration, or natural frequency would not eliminate the source of the damaging forces, and would be unlikely to prevent future failures. The valve flow geometry must be redesigned to create a more stable flow field. This is not a simple exercise, as was shown by the poor results from attempted quick fixes with the Mod 1 and Mod 2 valves. Furthermore, testing is required to verify the flow stability through a valve.

The hybrid valve discussed in this paper showed stable flow in tests and has performed without excessive vibration in all applications so far. The authors expect it to be reliable when installed in the turbine discussed in this paper and in all applications for the foreseeable future.

APPENDIX A —

PRESSURE PORT LABORATORY TEST

In order to clear insulation blankets, the pressure ports shown in Figure 6 had long lengths of piping with access valves to install static pressure gauges or transducers to measure nozzle ring pressures as valves are opened. However, some pressure transducers also can obtain dynamic pressures. For the turbine, strain-gauge transducers were used that also provide static pressures. Because the transducers are not flush-mounted, there will be an acoustic resonance having a quarter-wave length ($1/4$ of the length from the opening to the end of the piping where the transducer is located). In other words, this open-closed pipe will have a very small pulsation from the excitation of turbulent flow just at the port opening, a node, with maximum pressure pulsation at the closed end where the transducer is located. The equation from den Hartog (1954) for the frequency, F_1 , in Hz for the first open-closed mode is given by: $F_1 = V_A / (4 \cdot L)$ where V_A is gas acoustic velocity in ft/sec, and L is overall pipe length in feet. The diameter of the cavity has a small effect for long tubes, and the presence of the valve trim will also modify the frequency. The effective length for short tubes is $(L + 8D/3)$, where L is the length and D is the diameter.

A mockup of a port, valve, "pig-tail," and transducer was tested by blowing shop air past the 1 inch pipe port opening, as shown in Figure A-1. The pipe length to the access valve is about 17 inches, with another 38 inches to the transducer. Frequencies found for various test conditions are given in Table A-1. The equivalent frequencies for turbine inlet steam conditions are also given in the table. During testing, the resonance inside the port assembly could be heard inside the laboratory, as one would hear the resonance from organ pipes or blowing across the top of a bottle. The node for the mode is actually just inside the port. Tests were done to quantify the power of the open-closed "organ pipe" using a microphone measurement to obtain the sound power emanating from the port. For the air test, the ratio of pressure at the transducer at the end of the port to that 2.5 inches away, outside the port entrance, was near 200 to 1. Using this ratio for equivalent pressures to those for the turbine at conditions during severe vibration, calculations resulted in a sound power that would translate to about 5 psi peak pressure at the valve. In order to significantly reduce the high pul-

sations, plugs were designed to mate at the access flanges; the sound power with a small 1/8 inch diameter bore, 3.5 inches long at the port entrance, would be reduced by a factor of 40. Another test was done holding a microphone calibrator against the port opening with a 114 dB sound pressure level. Measurement at the closed access valve also gave 114 dB for a frequency well below the first mode of the closed-closed tube, showing that field data at 30 to 40 Hz would give accurate amplitudes.

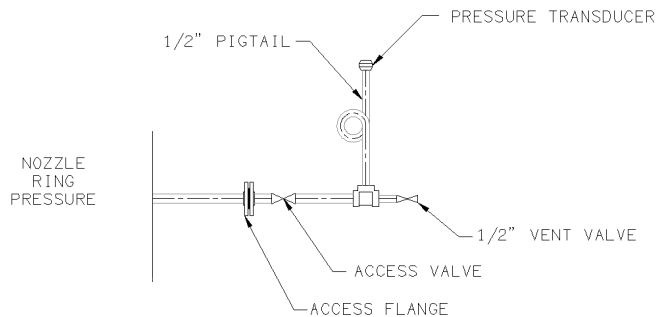


Figure A-1. Schematic of 1 Inch Pressure Port Including Vent Valve Used at Site.

Table A-1. Pressure Port Piping Mockup Test Results.

Configuration	Parameter	Result for Air Test	Predicted for Steam Conditions
Access valve closed	Frequency—Hz	224	430
Access valve open with only gas in pipe	Frequency—Hz	72	137
Access valve open with water in vertical run	Frequency—Hz	128	244
	Pressure at end of port—psi (rms)	0.28	NA
	Pressure near opening—psi (rms)	0.0015	NA

REFERENCES

- Araki, T., Okamoto, Y., and Ootomo, F., 1981, "Fluid-Induced Vibration of Steam Control Valves," *Toshiba Review*, 36, (7), ISSN 0372-0462, Tokyo Shibaura Electric Company, Kawasaki, Japan, pp. 648-656.
- den Hartog, J. P., 1954, *Mechanical Vibrations*, New York, New York: McGraw-Hill, pp. 277-280. (Reprint No. 647854 available from Dover Publications, Mineola, New York), p. 431.
- Feray, D. L., 1999, "A Rub in a High Speed Steam Turbine," Texas A&M Symposium, User Case Study #1, Twenty-Eighth Turbomachinery Symposium, Turbomachinery Laboratory, Texas A&M University, College Station, Texas.
- Glinka, G. and Newport, A., 1987, "Universal Features of Elastic Notch-Tip Stress Fields," *International Journal of Fatigue*, 9, (3), pp. 143-150.
- Glinka, G. and Shen, G., 1991, "Universal Features of Weight Functions for Cracks in Mode I," *Engineering Fracture Mechanics*, 40, (6), pp. 1135-1146.
- Heymann, F. J. and Staiano, M. A., 1973, "Steam Turbine Control Valve Noise," Engineering Report EM-1319, Westinghouse Electric Corporation, Lester, Pennsylvania.
- Johns, D. A., Rasmussen, D., and Beverly, J., 1997, "Turbine Remanufacture—One Option for Reliability and Efficiency Improvement," *Proceedings of the Twenty-Sixth Turbomachinery Symposium*, Turbomachinery Laboratory, Texas A&M University, College Station, Texas, pp. 104-105.
- Kurihara, M., Katoh, A., and Kawahara, M., 1987, "Effects of Stress Ratio and Step Loading on Fatigue Crack Propagation Rate," *Current Research on Fatigue Cracks*, Editors, Tanaka, M. Y. and Komai, K., Elsevier Applied Science, London, pp. 247-265.

ACKNOWLEDGEMENT

The authors would like to thank the Elliott Turbomachinery Company and DOW Chemical for allowing this paper to be published, as well as the numerous technical personnel at both companies who were involved in the troubleshooting and resolution of these valve failures.